Polyurethane Networks from Fatty-Acid-Based Aromatic Triols: Synthesis and Characterization

Gerard Lligadas, Joan C. Ronda, Marina Galià,* and Virginia Cádiz

Departament de Química Analítica i Química Orgànica, Universitat Rovira i Virgili, Campus Sescelades, Marcel.lí Domingo s/n, 43007 Tarragona, Spain

Received February 6, 2007; Revised Manuscript Received March 2, 2007

Novel biobased aromatic triols (1,3,5-(9-hydroxynonyl)benzene and 1,3,5-(8-hydroxyoctyl)-2,4,6-octylbenzene) were synthesized through the transition-metal-catalyzed cyclotrimerization of two alkyne fatty acid methyl esters (methyl 10-undecynoate and methyl 9-octadecynoate) followed by the reduction of the ester groups to give terminal primary hydroxyl groups. A series of biobased segmented polyurethanes based on these triols, 1,4-butanediol as a chain extender and 4,4′-methylenebis(phenyl isocyanate) as a coupling agent, were synthesized. Samples were prepared with hard-segment contents up to 50%. The morphologies and thermal properties of these polyurethanes were studied by Fourier transform infrared spectroscopy, wide-angle X-ray diffraction, differential scanning calorimetry, thermogravimetric analysis, and dynamic mechanical thermal analysis. Partial crystallinity and phase separation were detected in samples with hard-segment content of 50%.

Introduction

The petrochemicals that are used intensively in the worldwide chemical industry are limited resources that will be depleted within the foreseeable future, which has fueled efforts to find alternatives.[1] In the polyurethane industry, conventional polyether polyols, which account for 80% of the total worldwide consumption of oligopolyols, are mostly produced from petroleum-based alkylene oxides. Due to uncertainty about the future cost of petroleum as well as the desire to move toward more environmentally friendly feedstocks, many recent efforts have focused on replacing all or part of the conventional petroleum-based polyols with those made from renewable resources such as vegetable oils. Combined with isocyanates, vegetable-oil-based polyols produce polyurethanes that can compete in many ways with polyurethanes derived from petrochemical polyols, and their preparation for general polyurethane use has been the subject of many studies.[2−11] Moreover, due to the hydrophobic nature of triglycerides, vegetable oils produce polyurethanes that have excellent chemical and physical properties such as enhanced hydrolytic and thermal stability.[12,13] However, it is a challenge to synthesize suitable diisocyanates via diamino compounds derived from vegetable oils, making it possible to produce polyurethanes completely from renewables.[14]

Vegetable oils are one of the cheapest and most abundant biological sources available in large quantities, and their use as starting materials has numerous advantages: for example, low toxicity, inherent biodegradability, and high purity.[15] They are considered to be one of the most important classes of renewable resources for the production of biobased thermosetting polyurethanes.[16] For natural oils to be used as raw materials for polyol production, multiple hydroxyl functionality is required. Two different ways of preparing vegetable-oil-based polyols have been successfully developed. In the first, polyols are formed by reaction at the double bond of the unsaturated fatty oil. For example, the epoxidation and further oxirane ring opening leads to polyols with secondary hydroxyl groups,[6−8] while the hydroformylation and the ozonolysis lead to polyols with primary hydroxyl groups.[9,10] In the second, a combined reaction at the double bonds and subsequent reduction of the carboxyl group yields the hydroxyl-moieties.[11]

To further expand applications of these biorenewable materials, our group has focused on converting vegetable oils into useful polyurethanes.[11,17] After our efforts to functionalize vegetable oils, the introduction of aromatic comonomers into the polymer structure would appear to be suitable in the search for new viable polymeric materials. Aromatic compounds derived from fats can be obtained by transition-metal-catalyzed cyclotrimerization of the respective alkyne fatty derivatives.[18]

Herein, we report the synthesis and characterization of two biobased triols (UDT and OLT; Chart 1) prepared by the trimerization of methyl 10-undecynoate and methyl 9-octadecynoate, respectively. Both esters can be synthesized from 10-undecenoic acid and 9-octadecenoic acid, which can be obtained from castor oil and sunflower oil, respectively. Polyurethanes were obtained from these triols, butanediol as a chain extender, and 4,4′-methylenebis-(phenyl isocyanate). The chemical structures, molecular characteristics, and thermal properties were studied using Fourier transform infrared (FTIR) spectroscopy, wide-angle X-ray diffraction (WAXD), differential scanning calorimetry (DSC), dynamic mechanical thermal analysis (DMTA), and thermogravimetric analysis (TGA).

Experimental Section

Materials. The following chemicals were obtained from the sources indicated: Oleic and 10-undecenoic acids, purchased from Fluka, were used as received. Copper(II) chloride, $CuCl_2$ (97%, from Aldrich), palladium(II) chloride, $PdCl_2$ (99.9%, from Strem Chemicals), bromine (99%, from Aldrich), potassium hydroxide (90%, from Scharlau), chlorotrimethylsilane (97%, from Aldrich), trimethyl orthoformate (98%, from Fluka), Amberlist 15 (from Aldrich), palladium on carbon, Pd/C (10 wt %, from Aldrich), lithium aluminum hydride, $LiAlH_4$ (97%, from SDS), 1,4-butandiol, BD (99%, from Aldrich), and 4,4′-methylenebis(phenyl isocyanate) (MDI, from Aldrich)

* Author to whom correspondence should be addressed. E-mail: marina.galia@urv.cat.

10.1021/bm070157k CCC: $37.00
Published on Web 05/02/2007

Chart 1. Chemical Structures of Methyl-9-Octadecynoate- and Methyl-10-Undecynoate-Based Triols Obtained by Cyclotrimerization and Subsequent Reduction.

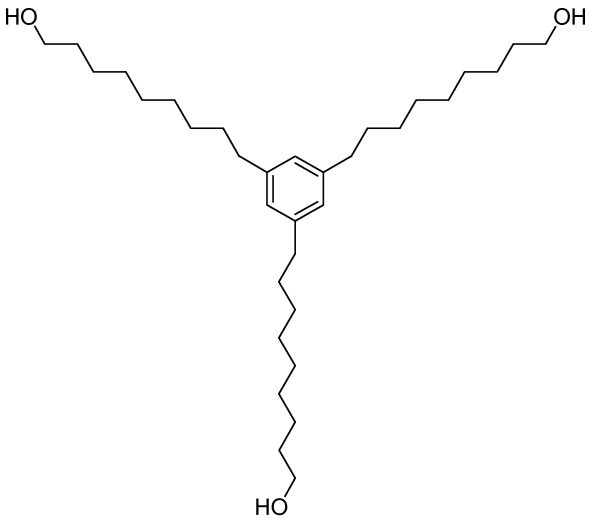

UDT

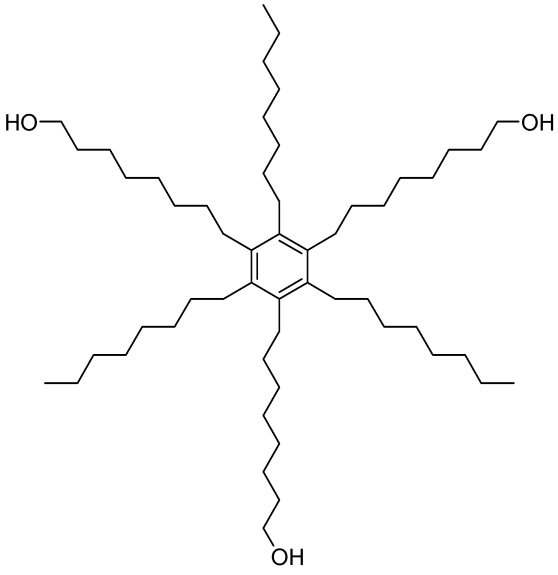

OLT

were all used as received. Tetrahydrofuran (THF) was distilled from sodium immediately before use. Other solvents were purified by standard procedures.

Synthesis of 10-Undecynoic Acid. A 1000 mL, two-necked, round-bottom flask provided with a Teflon-coated magnetic bar and a pressure-equalized dropping funnel was charged with 184.3 g (1 mol) of undecenoic acid and 500 mL of dry CCl_4. The flask was cooled in a cooling mixture of ice and water, the solution was stirred magnetically, and 167.8 g (54 mL, 1.05 mol) of dry bromine was added during a period of 1 h. The mixture was allowed to warm up gradually to room temperature, and after stirring overnight, the solvent and the excess of bromine were removed at reduced pressure. The brown liquid dibromo acid was transferred to a 1 L round-bottomed flask, and a solution of 200 g of potassium hydroxide in 600 mL of water was added. The mixture was heated at reflux temperature for 8 h, and a solution of 2 L of water with 100 mL of concentrated sulfuric acid was added. The product was extracted with several portions of ether and dried with anhydrous magnesium sulfate, and the ether was removed under reduced pressure. The residue was distilled under reduced pressure (0.5 mmHg) and the fraction at 120−130 °C was collected. The product solidifies on cooling and was recrystallized from hexane to obtain a white solid (yield 49%, mp 41−42 °C).

^{1}H NMR ($CDCl_3$/TMS, δ, ppm): 1.24−1.33 (m, 8H), 1.44 (m, 2H), 1.55 (m, 2H), 1.88 (s, 1H), 2.11 (m, 2H), 2.23 (t, 2H), 11.81 (s, 1H).

Synthesis of 9-Octadecynoic Acid. 9,10-Dibromooctadecanoic acid was obtained using a similar procedure as described above, but dehydrobromination was carried out using a solution of potassium hydroxide (112 g, 2 mol), 50 mL of water, and 400 mL of ethylene glycol monoethylether. The product was distilled under reduced pressure (0.5 mmHg), and the fraction at 196−200 °C was collected. The product solidifies on cooling and was recrystallized from hexane to obtain a white solid (yield 37%).

^{1}H NMR ($CDCl_3$/TMS, δ, ppm): 0.86 (t, 3H), 1.23−1.67 (m, 22H), 2.11 (m, 4H), 2.29 (t, 2H), 11.62 (s, 1H).

Synthesis of Methyl 10-Undecynoate and Methyl 9-Octadecynoate. A 500 mL round-bottomed flask was charged with 54.7 g (0.3 mol) of 10-undecynoic acid, 200 mL of methanol, 17 mL (15.9 g, 0.15 mol) of trimethyl orthoformate, and 2 g of Amberlist 15. The mixture was heated at reflux temperature for 4 h, resin was filtered, and 200 mL of ether was added. The solution was washed twice with water and dried with anhydrous magnesium sulfate, and the ether was removed under reduced pressure. Methyl 10-undecynoate was purified by fractionated distillation (4 mmHg, 96−98 °C) (yield 87%).

^{1}H NMR ($CDCl_3$/TMS, δ, ppm): 1.24−1.33 (m, 8H), 1.44 (m, 2H), 1.55 (m, 2H), 1.88 (s, 1H), 2.11 (m, 2H), 2.23 (t, 2H), 3.59 (s, 3H).

Methyl 9-octadecynoate was prepared by the same procedure starting from 42 g (0.15 mol) of 9-octadecynoic acid. The product was purified by fractionated distillation (0.5 mmHg, 125−130 °C) (yield 93%).

^{1}H NMR ($CDCl_3$/TMS, δ, ppm): 0.86 (t, 3H), 1.23−1.67 (m, 22H), 2.11 (m, 4H), 2.29 (t, 2H), 3.65 (s, 3H).

Synthesis of 1,3,5-(9-Hydroxynonyl)benzene (UDT). Palladium(II) chloride (0.26 g, 1.5 mmol), copper(II) chloride (7.1 g, 52.8 mmol), 260 mL of benzene, and 15 mL of butanol were placed in a 500 mL, two-necked flask equipped with a thermometer, dropping funnel, condenser, and Teflon-coated magnetic stir bar. The temperature was gradually brought to 40 °C, and methyl 10-undecynoate (5 g, 25.5 mmol) was added dropwise. The resulting mixture was stirred for 5 h. The progress of the reaction was monitored by thin-layer chromatography with hexane/ethyl acetate (9:1) as the eluent. Once the reaction was finished, the resulting mixture was cooled to room temperature and passed through a celite column, and the solvents were evaporated off. The crude product was dissolved in 50 mL of anhydrous THF and added dropwise to a dispersion of lithium aluminum hydride (6.6 g, 179.3 mmol) in 400 mL of anhydrous tetrahydrofuran. After the addition was complete, the mixture was stirred vigorously at room temperature for 1 h, and then the excess $LiAlH_4$ was decomposed by adding 50 mL of ethyl acetate dropwise. A 10% H_2SO_4 aqueous solution was added, and the aqueous layer was extracted with ethyl acetate. The combined organic phase was washed with a saturated sodium bicarbonate solution ($NaHCO_3$) until the pH was neutral, washed with brine, dried over anhydrous magnesium sulfate, and filtered, and the solvent was evaporated off to yield a white powder. The product was then purified by flash chromatography with a silica gel column and hexane/ethyl acetate (8:1) as the eluent. When the solvent was removed, 3.0 g of pure UDT (yield 70%) was obtained as a white powder.

^{1}H NMR ($CDCl_3$/TMS, δ, ppm): 1.23−1.59 (m, 42H), 2.37 (t, 6H), 3.60 (t, 6H), 6.38 (s, 3H).

^{13}C NMR ($CDCl_3$, δ, ppm): 25.86 (t), 27.60 (t), 28.72 (t), 29.40 (t), 29.52 (t), 29.59 (t), 32.87 (t), 40.00 (t), 63.05 (t), 120.48 (d), 137.79 (s).

Synthesis of 1,3,5-(8-Hydroxyoctyl)-2,4,6-octylbenzene (OLT). *Cyclotrimerization of Methyl 9-Octadecynoate.* A 50 mL, two-necked, round-bottom flask equipped with a Teflon-coated magnetic stir bar and a pressure-equalized dropping funnel was charged with trimethylsilyl chloride (2.5 mL, 0.019 mmol), palladium on carbon (Pd/C) (10 wt %, 0.65 g), and 10 mL of THF. To this solution, methyl 9-octadecynoate (5 g, 17.0 mmol) was added dropwise with stirring at room temperature for 1 h. The temperature was raised and maintained

Table 1. Chemical Composition of Polyurethane Networks

sample code[a]	polyol (g)	BD (g)	MDI (g)	% hard segment[b]
OLT−PU	1	0	0.49	
OLT−PU44	1	0.077	0.71	44.0
OLT−PU52	1	0.15	0.93	51.9
UDT−PU	1	0	0.77	
UDT−PU45	1	0.015	0.81	45.2
UDT−PU52	1	0.083	1.00	51.9

[a] The number in the sample code denotes the hard-segment wt % of the PU. [b] The hard-segment percentage is calculated as the wt % of BD and MDI per total material weight.

under reflux for about 5 h. The progress of the reaction was monitored by thin-layer chromatography with hexane/ethyl acetate (3:1) as the eluent. The resulting mixture was cooled to room temperature, filtered, and the excess of tetrahydrofurane was evaporated off. The yellow oil obtained was purified by flash chromatography with silica gel column and hexane/ethyl acetate (15:1) as the eluent. When the solvent was removed, 3.6 g of pure product (yield 72%) was obtained as a viscous oil.

^{1}H NMR ($CDCl_3$/TMS, δ, ppm): 0.9 (t, 9H), 1.25−1.70 (m, 72H), 2.32 (t, 6H), 2.48 (m, 12H), 3.68 (s, 9H).

^{13}C NMR ($CDCl_3$, δ, ppm): 14.27 (q), 22.83 (t), 25.10 (t), 29.21 (t), 29.32 (t), 29.47 (t), 29.89 (t), 30.49 (t), 30.63 (t), 30.80 (t), 31.62 (t), 31.71 (t), 32.08 (t), 34.21 (t), 51.53 (q), 136.8 (s), 174.3 (s).

Reduction of 1,3,5-(8-Methoxycarbonyloctyl)-2,4,6-octylbenzene. Lithium aluminum hydride (4.2 g, 114 mmol) was dispersed in 250 mL of anhydrous THF in a 250 mL, two-necked, round-bottomed flask under argon atmosphere. The ester derivative (3.6 g, 4.1 mmol), dissolved in anhydrous THF (25 mL), was added dropwise with stirring over a period of 30 min. After addition was complete, the mixture was stirred vigorously at room temperature for 1 h. After this, the excess $LiAlH_4$ was decomposed by adding 50 mL of ethyl acetate dropwise. Then, 10% H_2SO_4 aqueous solution was added, and the aqueous layer was extracted with saturated sodium bicarbonate solution ($NaHCO_3$) until the pH was neutral and brine. The organic phase was dried over anhydrous magnesium sulfate and filtered, and the solvent was evaporated off yielding a viscous liquid (3.2 g, 98%).

^{1}H NMR ($CDCl_3$/TMS, δ, ppm): 0.89 (t, 9H), 1.25−1.59 (m, 72H), 2.47 (m, 12H), 3.64 (t, 6H).

^{13}C NMR ($CDCl_3$/TMS, δ, ppm): 14.30 (q), 22.86 (t), 25.93 (t), 29.46 (t), 29.48 (t), 29.51 (t), 29.61 (t), 29.90 (t), 30.75 (t), 30.83 (t), 30.93 (t), 31.61 (t), 32.09 (t), 32.10 (t), 32.90 (t), 63.00 (t), 136.8 (s).

Synthesis of Polyurethanes. Polyurethanes were prepared using a single-stage process. After 5 min of mixing the appropriate amount of polyol (OLP or UDP) and chain extender (BD) at 75 °C, diisocyanate (MDI) at a NCO/OH ratio of 1.02 was added, and then additional mixing for 30 s was conducted. The mixture was cured for 2 h at 75 °C and then postcured at 110 °C overnight. Chemical composition and hard-segment content of the polyurethanes are shown in Table 1. From the sample code in Table 1, the numbers denote the hard-segment percentage of the polyurethanes.

Characterization. The NMR spectra of the oil samples were recorded on a Varian Gemini 400 MHz spectrometer (400 MHz for ^{1}H and 100.57 MHz for ^{13}C). The samples were dissolved in deuterated chloroform, and ^{1}H NMR and ^{13}C NMR spectra were obtained at room temperature using TMS as the internal standard. The IR spectra were recorded on a Bomem Michelson MB 100 FTIR spectrophotometer with a resolution of 4 cm^{-1} in absorbance mode. An attenuated total reflection (ATR) accessory with thermal control and a diamond crystal (Golden Gate heated single-reflection diamond ATR, Specac-Teknokroma) was used to determine FTIR spectra.

Calorimetric studies were carried out on a Mettler DSC822e thermal analyzer with N_2 as the purge gas. The heating rate was 20 °C/min. T_g was determined from the second heating scan of DSC measurements as the temperature of the halfway point of the jump in the heat capacity. Thermal stability studies were carried out on a Mettler TGA/SDTA851e/LF/1100 with N_2 as the purge gas at scanning rates of 10 °C/min.

WAXD measurements were made using a Siemens D5000 diffractometer (Bragg−Brentano parafocusing geometry and vertical $\theta-\theta$ goniometer) fitted with a curved graphite diffracted-beam monochromator, incident- and diffracted-beam Soller slits, a 0.06° receiving slit, and scintillation counter as a detector. The angular 2θ diffraction range was between 1° and 40°. Samples were dusted onto a low background Si(510) sample holder. The data were collected with an angular step of 0.05° at 3 s per step. Cu Kα radiation was obtained from a copper X-ray tube operated at 40 kV and 30 mA.

Mechanical properties were measured with a dynamic mechanical thermal analyzer (TA DMA 2928). Specimens 1.2 mm thick, 5 mm wide, and 5 mm long were tested in a three-point bending configuration. The various thermal transitions were studied between −100 and 150 °C at a heating rate of 2.5 °C/min and a fixed frequency of 1 Hz.

Results and Discussion

Synthesis of Biobased Triols. Biobased triols UDT and OLT were synthesized in two steps: cyclotrimerization of methyl 10-undecynoate and methyl 9-octadecynoate to obtain the aromatic derivatives and subsequent reduction of carboxylate groups to give primary hydroxyl groups. Alkyne fatty derivatives were obtained in moderate yields from the corresponding fatty acids by bromation, dehydrobromination, and esterification using well-established procedures[19] (Scheme 1). Dehydrobromination of the 9-octadecenoic acid derivative was carried out using a mixture of ethylene glycol monoethylether and water as a solvent. However, when dehydrobromination of the 10-undecenoic acid derivative was carried out in the same conditions, isomerization of the terminal triple bond was observed, and 9-undecynoic acid was obtained as a major product. The reaction was then carried out at lower temperature using water as a solvent, and the expected product was obtained in moderate yield.

Transition-metal-catalyzed cyclotrimerization of alkynes can be considered as one of the most powerful and general methodologies used to assemble arene rings, and a large number of transition metal catalyst have been developed for alkyne cyclotrimerization in organic media.[20] A simple method utilizes heterogeneous Pd/C catalyst in normal atmosphere with refluxing THF as the solvent and commercial grade trimethylsilylchloride.[21] Cyclotrimerization of methyl 9-octadecynoate was carried out following this procedure, and the formation of the aromatic derivative was confirmed by the appearance of the signal at 136.8 ppm in the ^{13}C NMR spectrum corresponding to the aromatic core. It has to be considered that trimerization of this unsymmetrical alkyne can produce the symmetric and the nonsymmetric trimer.[21] A clear preference for the formation of the kinetic product has been described, but the thermodynamic product could also be isolated. In our case, we presume that both compounds were formed. These two compounds could not be separated by flash chromatography due to their similar polarities. Therefore, the presence of two compounds cannot be ruled out.

The attempt to cyclotrimerize methyl 10-undecynoate in the same conditions as above-described resulted in the formation of polymeric material. No indication of trimer formation was obtained by NMR. This result indicates that the more reactive terminal alkyne undergoes polymerization much more readily than the disubstituted alkyne. The preparation of benzene derivatives via palladium-chloride-catalyzed cyclotrimerization of alkynes in the presence of $CuCl_2$ has been described as a smooth and regioselective method.[22] When we applied the

Scheme 1. Synthesis of (a) Methyl-9-Octadecynoate- and (b) Methyl-10-Undecynoate-Based Triols.

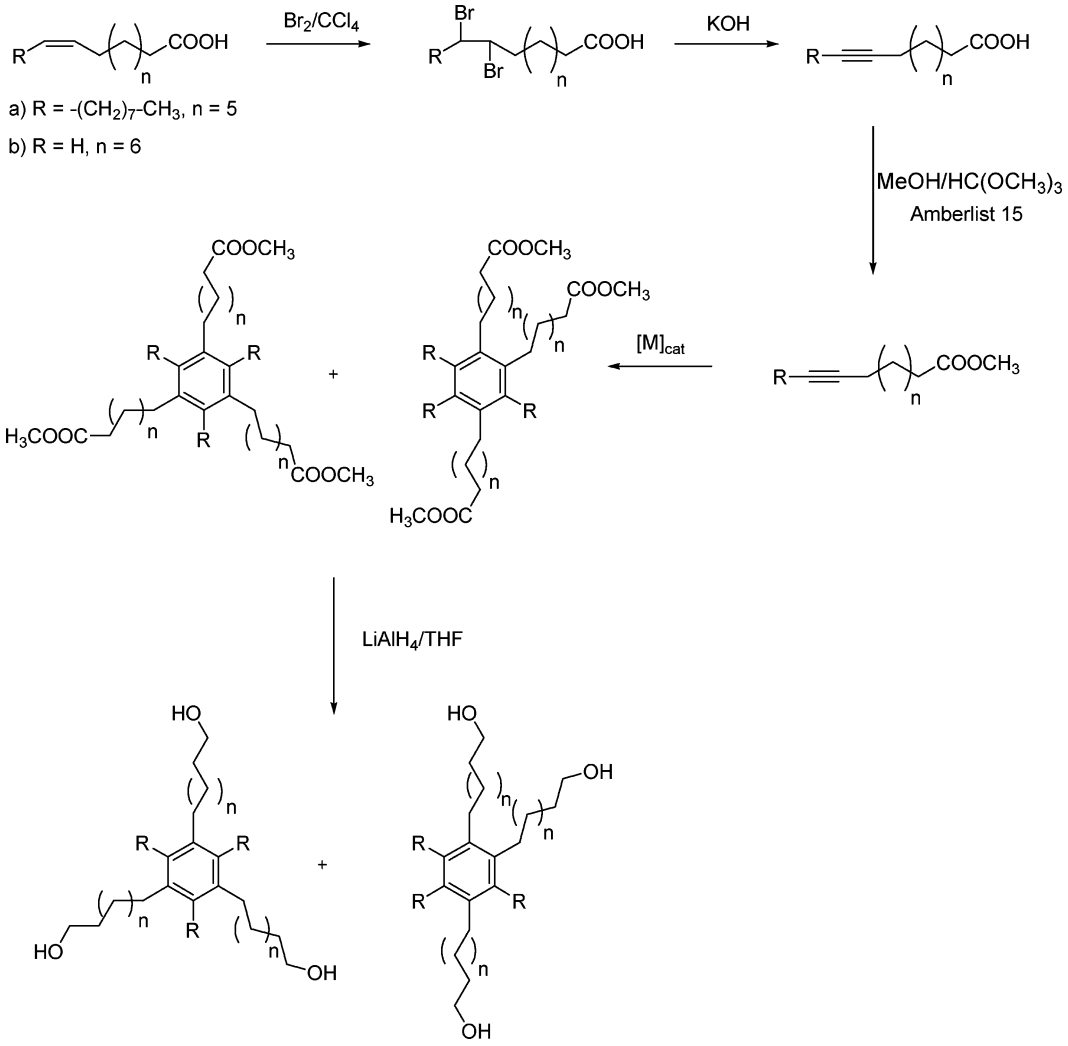

reaction to methyl 10-undecynoate, only a 1,3,5-trisubstituted benzene derivative was obtained regioselectively in a moderate yield. The appearance of signals at 6.38 ppm in the ^{1}H NMR spectrum and 120.48 and 137.79 ppm in the ^{13}C NMR spectrum confirms the formation of the symmetric product. A small amount of butyl ester was detected due to the use of butanol as the solvent that can cause transesterification. If methanol is used instead of butanol to avoid this problem, then cyclotrimerization is not observed. So, the former mixture of esters was used in the subsequent reduction step.

Aromatic ester derivatives were used as the starting material for the reduction of the carboxylate groups to synthesize two triols with primary hydroxyl groups. The reduction was carried out using lithium aluminum hydride as a reducing agent in THF solution, and the expected products were characterized by NMR. Figure 1 shows the ^{1}H and ^{13}C NMR spectra of OLT with all of the signal assignments. The thermal behavior of both polyols was investigated by DSC. OLT, obtained as a yellow, viscous oil, showed a glasslike transition with an end point at −49 °C while UDT, obtained as a crystalline solid, showed a melting point at 72 °C. WAXD pattern of UDT confirmed calorimetric findings, displaying well-defined peaks according to an ordered crystalline structure.

Synthesis and Characterization of Polyurethanes. Vegetable-oil-based polyols have been widely used to produce segmented and nonsegmented polyurethanes.[2−11,23] Segmented polyurethanes are elastomeric block copolymers that generally exhibit a phase-segregated morphology made up of soft rubbery segments and hard glassy or semicrystalline segments.[24] The soft segment usually consists of polyether or polyester diols whereas the hard segment consists of the diisocyanate component and a low molecular weight chain extender. The advantage of segmented polyurethanes is that their segmental and domain structure can be controlled over a considerable range through the selection of the materials, their relative proportions, and the processing conditions.

In this study, biobased polyurethanes were prepared using the one-shot technique from UDT or OLT, BD as a chain extender, and MDI as a coupling agent. The biobased triol/MDI part is considered the soft phase even though its glass transition is above room temperature (Table 1). The MDI/BD hard segments are more rigid than the MDI/triol matrix. These hard segments are polar, crystallizable and likely to form a separate phase if the hard-segment content is high enough. The chemical composition and hard-segment content of the synthesized polyurethanes are shown in Table 1. The NCO/OH molar ratio was kept at 1.02 to compensate for isocyanates that are consumed in side reactions during the urethane synthesis. Reactants were mixed at 75 °C and cured at this temperature for 2 h and postcured at 110 °C overnight to give the polyurethanes. The conversion of the isocyanate groups to urethane linkages was monitored by the disappearance in the IR spectra of the adsorption band at 2240 cm^{-1} assigned to the

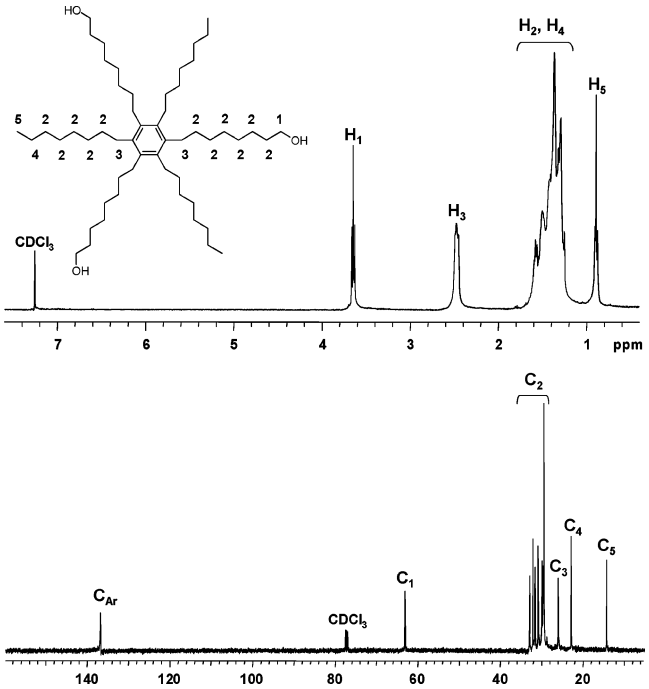

Figure 1. ^{1}H and ^{13}C NMR spectra of methyl 9-octadecynoate-based triol (OLT).

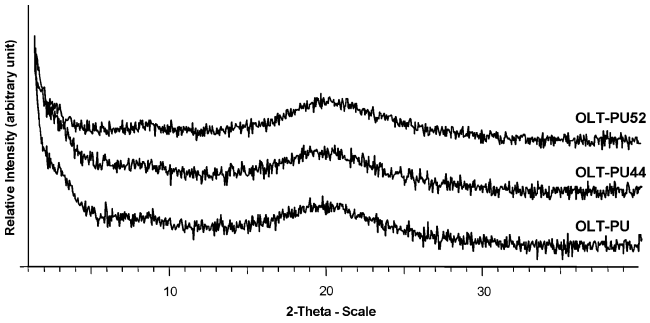

Figure 2. WAXD data of OLT-based polyurethanes.

isocyanate group and the appearance of a new band at 1700 cm^{-1} assigned to the urethane bond.

To investigate the molecular structure of polyurethanes WAXD and FTIR were employed. All samples show similar WAXD curves with a broad halo characteristic of amorphous substances with the maximum at about $2\theta = 20°$. In Figure 2 WAXD profiles of OLT-based polyurethanes are shown. The WAXD curves for extended polyurethanes show essentially the same pattern as those for the nonextended samples, indicating little crystallization. FTIR spectroscopy was used to investigate the structural differences in hard and soft segments of synthesized polyurethanes with OLT or UDT and various BD fractions. Almost all the infrared research on polyurethanes has focused on two principal vibrational regions: the N−H stretching vibration (3200−3500 cm^{-1}) and the carbonyl C═O stretching vibration amide I region (1700−1730 cm^{-1}). Polyurethanes are capable of forming several kinds of hydrogen bonds due to the presence of a donor N−H group and a C═O acceptor group in the urethane linkage. Therefore, hard segment−hard segment or hard segment−soft segment hydrogen bonding can exist. These bands have been widely used to characterize, at least semiquantitatively, the hydrogen bonding state of the polymer, and to correlate this to the phase separation in the system.[25,26] It is well-known that in hydrogen-bonded urethane N−H and C═O bands appear at lower wavenumbers than that those in free ones.[27] Figure 3 shows the FTIR spectra of the C═O

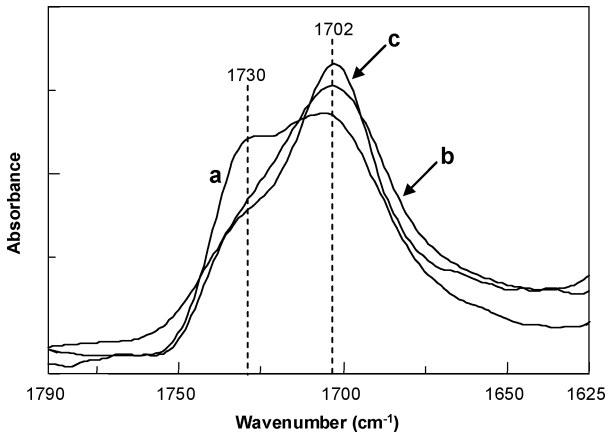

Figure 3. FTIR spectra of the carbonyl region of OLT-based polyurethanes: (a) OLT−PU, (b) OLT−PU44, and (c) OLT−PU52.

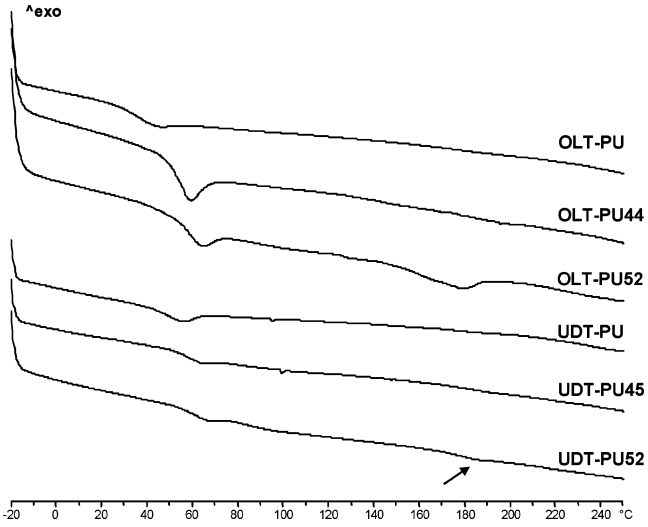

Figure 4. DSC thermograms (20 °C/min) of OLT- and UDT-based polyurethanes.

stretching vibration region for OLT-based polyurethanes. The broad band between 1750 and 1650 cm^{-1} is attributable to associated and nonassociated C═O urethane groups. Analysis of this stretching vibration for the polyurethane (PU) sample indicates that there is a band at approximately 1730 cm^{-1} attributable to free C═O urethane groups and a band at about 1702 cm^{-1} that is due to the hydrogen-bonded C═O urethane. The intensities of the bands attributed to free and hydrogen-bonded urethane carbonyls are similar, but the intensity of the band attributed to hydrogen-bonded urethane, relative to the band attributed to the nonbonded urethane groups, increases with an increase in the hard-segment content. Therefore, OLT−PU52 and OLT−PU44 C═O urethane groups are hydrogen-bonded to a greater degree than those in the OLT−PU sample. A similar behavior was observed for UDT-based polyurethanes. The difference in the state of molecular aggregation of polyurethanes was further confirmed by DSC.

Thermal Properties of Polyurethanes. Thermal analysis of the polyurethanes obtained was performed to provide insights into the morphological structure of the material. Figure 4 shows the DSC thermogram for the polyurethanes, and thermal transitions are listed in Table 2. No melting or crystallization peaks were found by DSC for OLT−PU, which is in full agreement with the WAXD observation. The glass transition temperature of this reference sample measured by DSC was 36 °C. DSC thermograms of the OLT-based polyurethanes extended with BD showed a glass transition, indicated by an

Table 2. Thermal Characterization of Polyurethane Networks from DSC, DMTA, and TGA

		DSC (°C)			DMTA		TGA (°C)	
sample code[a]	% hard segment[b]	T_g (°C)	T_m (°C)	ΔH_m (J/g)	tan δ_{max}[c] (°C)	$E'_{20°C}$ (MPa)	$T_{5\%\ loss}$[d]	T_{max}[e]
OLT−PU		36			56	5.0	327	381/461
OLT−PU44	44.0	53			64	2.4	308	316/458
OLT−PU52	51.9	58	177	3.2	74	4.2	288	348/455
UDT−PU		48			62	7.0	331	377/470
UDT−PU45	45.2	59			87	6.3	315	350/466
UDT−PU52	51.9	61	183	0.6	89	4.5	290	325/465

[a] The number in the sample code denotes the hard-segment wt % of the PU. [b] The hard-segment percentage is calculated as the wt % of BD and MDI per total material weight. [c] Maximum value of the tan δ temperature curve from DMTA. [d] Temperature of 5% weight loss. [e] Temperature of the maximum weight loss rate.

endothermic step in the heat flow. Such transitions appeared in the region from 53 to 58 °C and were attributed to the OLT soft-segment glass transition temperature (T_g). The T_g value is a measure of relative purity of the soft-segment regions; when there are hard segments dispersed in the soft domains, the T_g is raised. The addition of bifunctional components such as MDI/BD reduces cross-linking density but increases phenyl ring content. In principle, reduced cross-linking density should decrease the T_g, but increased aromatic content should have the opposite effect. Apart from this, the sample with higher hard-segment content (OLT−PU52) revealed a melting endotherm centered at 177 °C associated with hard-segment domains, which supports the development of a phase-separated morphology and indicates that hard-segment content is high enough to achieve phase separaration. WAXD apparently is not sensitive enough to detect the crystalline fractions in the largely amorphous matrix of the OLT−PU52 sample. In a second DSC scan after melting, no melting peaks were observed, which is probably due to miscibility of the hard and soft segments above the melting point. High viscosity and low mobility due to the cross-linking make the crystallization upon curing difficult. In the case of UDT−PU, only a glass transition can be observed in the DSC thermogram at 48 °C. This value is higher than the one for OLT−PU, which can be explained from several factors including: (a) the plasticizing effect of long aliphatic chains that remain elastically inactive even at full conversion of functional groups and (b) differences in composition of the networks (i.e., the higher content of MDI in UDT-based polyurethanes (43 vs 32 wt %), which increases the stiffness of the network structure). UDT−PU45 shows only a glass transition in the DSC thermogram, while in the DSC thermogram of UDT−PU52 a small endotherm appears, meaning that phase mixing is more likely than phase separation in the case of UDT. The degree of hard-segment mixing into the soft-segment domain will depend on the overall hard-segment content and the affinity of one segment toward the other. In UDT−polyurethanes, hard-segment content is similar to that of the OLT−polyurethanes, but the soft segment exhibits higher polarity and a higher affinity to the hard phase. The experimental glass transition temperatures revealed that the dispersion of hard segments in the soft domain increased with the hard-segment content, as in the OLT−polyurethanes.

TGA is the most favored technique for the evaluation of the thermal stability of polymers. Polyurethanes have relatively low thermal stability, mainly because the presence of urethane bonds. From the derivative curves it can be seen that in nitrogen more than one process occurs during thermal degradation (Table 2). Petrovic et al.[12] observed a similar behavior in the case of vegetable-oil-based polyurethanes. They showed that poly(oxypropylene)-based polyurethanes degrade in a single step, whereas vegetable-oil-based polyurethane show a two-step decomposition. The first degradation step, at temperatures between 300 and 400 °C, can be associated with the decomposition of urethane bonds, which takes place through the dissociation to isocyanate and alcohol, the formation of primary amines and olefins, or the formation of secondary amines.[28] This weight loss increases and occurs at lower temperatures as the hard-segment content increases, which is in accordance with the existence of a higher amount of weaker urethane bonds. The main degradation process can be observed at temperatures around 450 °C.

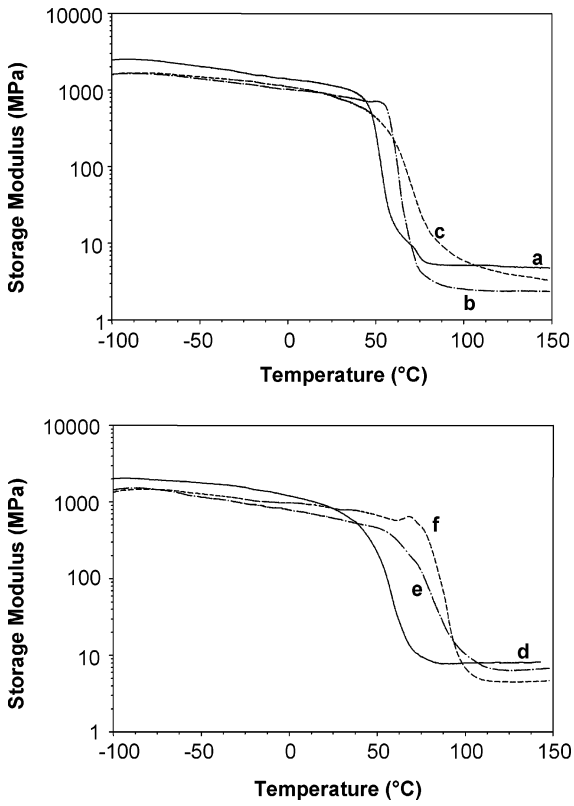

Figure 5. DMTA dynamic storage moduli (E') plots as a function of temperature for (a) OLT−PU, (b) OLT−PU44, (c) OLT−PU52, (d) UDT−PU, (e) UDT−PU45, and (f) UDT−PU52.

The dynamic mechanical behavior of the prepared polyurethanes was obtained as a function of the temperature beginning in the glassy state to the rubbery plateau of each material. Changes in the storage modulus (E') with temperature, obtained from DMTA on the OLT- and UDT-based polyurethane samples, carried out at the frequency of 1 Hz, are shown in Figure 5. DMTA enables T_g of the cross-linked materials to be determined. It is detected as the α-relaxation peak of the loss factor (tan δ), which corresponds to the transition midpoint of the log of the E' curve. The T_g values of the polyurethanes determined by DMTA are listed in Table 2. These values are higher than the values obtained by DSC, which can be related

to the heat transporting hysteresis for the large-scale sample in DMTA. From the DMTA curves, the plateau of E' in the rubbery state can be used to make qualitative comparisons of the level of cross-linking among the different polyurethanes. The addition of bifunctional components such as MDI/BD into thermosetting polyurethanes reduces cross-link density. In principle, reduced cross-link density should decrease E' at a rubbery state. In the case of OLT-based polyurethanes, in the rubbery region E' for OLT−PU52 is higher than that for OLT−PU44, although the latter should have higher cross-linking density, due to the existence of crystalline domains. Therefore, it appears that the hard segments play the role of physical cross-links and fillers. For UDT-based polyurethanes, E' follows the expected trends and decreases as the hard-segment content increases. It can be seen from Figure 5 that several samples show a slight increase in E' at the onset of T_g. Such behavior is explained by the nonequilibrium state of the material, possibly due to the fast cooling, resulting in frozen high free volume. Such materials display densification (volume shrinkage) with heating at the onset of T_g, resulting in modulus increase.[23]

Conclusions

Novel biobased aromatic triols, OLT and UDT, were synthesized by the transition-metal-catalyzed cyclotrimerization of methyl 10-octadecynoate and methyl 10-undecynoate respectively, followed by the reduction of the ester groups to primary alcohols. OLT was obtained as a viscous oil, while UDT exhibited a high tendency to crystallize at room temperature. The corresponding polyurethane networks with hard-segment content up to 52% were prepared by the reaction of the polyol, BD, and MDI. The synthesized materials were characterized by spectroscopic techniques, WAXD, DSC, TGA, and DMTA.

Partial crystallinity and phase separation were detected in samples with hard-segment content of about 50%, but they were not discernible in samples with low hard-segment content. In UDT-based polyurethanes the soft segment exhibits higher polarity and a higher affinity to the hard phase, meaning that phase mixing is more likely than phase separation. Phase separation was higher in OLT−PU52. Although the presence of hard segments lowers the cross-link density, samples with higher hard-segment content had higher T_g's, revealing dispersion of hard segments in the soft phase. These results show that it is possible to exploit renewable resources to manufacture original and useful materials.

Acknowledgment. The authors gratefully acknowledge the Comisión Interministerial de Ciencia y Tecnología (Grant No. MAT2005-01593) for financial support for this work and the Departament d'Universitats, Recerca i Societat de la Informació, and the Fons Social Europeu for a predoctoral grant (2003FI00765) to G.L.

References and Notes

(1) *Feedstocks for the Future: Renewables for the Production of Chemicals and Materials*; Bozell, J. J., Patel, M., Eds.; ACS Symposium Series 921; American Chemical Society: Washington, DC, 2006.
(2) Petrovic, Z. S.; Guo, A.; Javni, I. U. S. Patent 6,107,433, 2000.
(3) Kluth, H.; Gruber, B.; Meffert, B.; Huebner, W. U. S. Patent 4,-742,087, 1988.
(4) Hoefer, R.; Gruber, B.; Meffert, A.; Gruetzmacher, R. U. S. Patent 4,826,944, 1989.
(5) Suresh, K. I.; Kishanprasad, V. S. *Ind. Eng. Chem. Res*. **2005**, *44*, 4504.
(6) Guo, A.; Cho, Y.-J.; Petrovic, Z. S. *J. Polym. Sci., Part A: Polym. Chem.* **2000**, *38*, 3900.
(7) Zlatanic, A.; Petrovic, Z. S.; Dusek, K. *Biomacromolecules* **2002**, *3*, 1048.
(8) Zlatanic, A.; Lava, C.; Zhang, W.; Petrovic, Z. S. *J. Polym. Sci., Part B: Polym. Phys.* **2004**, *42*, 809.
(9) Guo, A.; Demydov, D.; Zhang, W.; Petrovic, Z. S. *J. Polym. Environ.* **2002**, *10*, 49.
(10) Petrovic, Z.; Zhang, W.; Javni, I. *Biomacromolecules* **2005**, *6*, 713.
(11) Lligadas, G.; Ronda, J. C.; Galià, M.; Biermann, U.; Metzger, J. O. *J. Polym. Sci., Part A: Polym. Chem.* **2006**, *44*, 634.
(12) Javni, I.; Petrovic, Z.; Guo, A.; Fuller, R. *J. Appl. Polym. Sci.* **2000**, *77*, 1723.
(13) Guo, A.; Javni, I.; Petrovic, Z. *J. Appl. Polym. Sci.* **2000**, *77*, 467.
(14) Metzger, J. O.; Bornscheuer, U. *Appl. Microbiol. Biotechnol.* **2006**, *71*, 13.
(15) (a) Baumann, H.; Bühler, M.; Fochem, H.; Hisrsinger, F.; Zoeblein, H.; Falbe, J. *Angew. Chem., Int. Ed. Engl.* **1988**, *27*, 41. (b) Biermann, U.; Friedt, W.; Lang, S.; Lühs, W.; Machmüller, G.; Metzger, J. O.; Klaas, M. R.; Schäfer, H. J.; Schneiderüsch, M. P. *Angew Chem., Int. Ed.* **2000**, *39*, 2206.
(16) (a) Andjelkovic, D. D.; Larock, R. C. *Biomacromolecules* **2006**, *7*, 927. (b) Tsujimoto, T.; Uyama, H.; Kobayashi, S. *Macromolecules* **2004**, *37*, 177, (c) Eren, T.; Küsefoglu, S. H. *J. Appl. Polym. Sci.* **2004**, *91*, 2700. (d) Khot, S. N.; LaScala, J. J.; Can, E.; Morye, S. S.; Williams, G. I.; Palmese, G. R.; Küsefoglu, S. H.; Wool, R. P. *J. Appl. Polym. Sci.* **2001**, *82*, 703. (e) Güner, F. S.; Yagci, Y.; Erciyes, T. *Prog. Polym. Sci.* **2006**, *31*, 633.
(17) (a) Lligadas, G.; Ronda, J. C.; Galià, M.; Cádiz, V. *Biomacromolecules* **2007**, *8*, 686. (b) Lligadas, G., Ronda, J. C.; Galià, M.; Cádiz, V. *Biomacromolecules* **2006**, *7*, 2420.
(18) Biermann, U.; Metzger, J. O. *Top. Catal.* **2004**, *27*, 119.
(19) *Vogel's Textbook of Practical Organic Chemistry*, 5th ed.; Furniss, B. S., Hannaford, A. J., Smith, P. W. G., Tatchell, A. R., Eds.; Longman Scientific & Technical: Harlow, 1989.
(20) Saito, S.; Yamamoto, Y. *Chem. Rev.* **2000**, *100*, 2901.
(21) Jhingan, A. K.; Maier, W. F. *J. Org. Chem.* **1987**, *52*, 1161.
(22) Li, J.; Jiang, H.; Chen. M. *J. Org. Chem.* **2001**, *66*, 3627.
(23) Petrovic, Z.; Cevallos, M. J.; Javni, I.; Schaefer, D. W.; Justice, R. *J. Polym. Sci., Part B: Polym. Phys.* **2005**, *43*, 3178.
(24) Wirpsza, Z. *Polyurethanes, Chemistry, Technology and Applications*; Kemp, T. J., Ed.; Ellis Horwood PTR Prentice Hall: New York, 1993.
(25) Skrovanek, D. J.; Howe, S. E.; Painter, P. C.; Coleman; M. M. *Macromolecules* **1985**, *18*, 1676.
(26) Papadimtrakopoulos, F.; Sawa, E.; MacKnight, W. J. *Macromolecules* **1992**, *25*, 4682.
(27) Seymour, R. W.; Estes, G. M.; Cooper, S. L. *Macromolecules* **1970**, *3*, 579.
(28) Levchik, S. V.; Weil, E. D. *Polym. Int.* **2004**, *53*, 1585.

BM070157K